



# Shaft Resistance of Displacement Piles in Overconsolidated Cohesionless Soils

Yasir M. Alharthi<sup>1,2(✉)</sup> and Adel M. Hanna<sup>1</sup>

<sup>1</sup> Department of Building, Civil and Environmental Engineering,  
Concordia University, 1455 de Maisonneuve Blvd. W., Montreal, QC H3G 1M8,  
Canada

harthiym@hotmail.com

<sup>2</sup> Department of Civil Engineering, Taif University, P.O. Box 888, Taif 2197,  
Saudi Arabia

**Abstract.** The conventional theories for predicting the capacity of a single pile in sand produce wide range of discrepancies. This is mainly due to the complexity of modeling cohesionless material, collecting field data, and ignoring the effect of overconsolidation in cohesionless soils.

This paper presents an experimental investigation on the capacity of closed-ended displacement piles (CEDP) in overconsolidated cohesionless soils with an emphasis on the shaft resistance. A large testing tank was instrumented to measure the overconsolidation ratio in the laboratory sand bed of homogeneous loose, medium, and dense sands. Tests were conducted on a long model pile at various embedment depths.

The resulted shaft resistance was found to be much higher than that calculated using conventional methods for homogeneous sand. By incorporating the overconsolidation ratio in the design, unique values were obtained for the shaft resistance of these piles.

The results of this experimental investigation are presented in the form of the measured shear stress along the pile's shaft and its unique distribution along its shaft. The critical depth for piles in cohesionless soils will be also addressed.

**Keywords:** Displacement piles · Shaft resistance · Stress distribution  
Critical depth · Overconsolidation ratio (OCR) · Sand  
Experimental investigation

## 1 Introduction

Piles are structural members that transfer the applied load of superstructures to deep supportive layers of soil or bedrock to provide sufficient support both axially and laterally. Conventional theories for predicting the shaft resistance of a single pile in sand have generated a range of discrepancies (Hanna and Nguyen 2002; Poulos and Davis 1980). This is due to the complexity of modeling cohesionless materials and collecting field data (Randolph et al. 1994).

In addition, the role of overconsolidation in such soils is often neglected. Whether occurring naturally or artificially, overconsolidation in cohesionless soils directly affects the lateral earth pressure that acts upon the pile shafts and thus upon pile

capacity. Overconsolidation can occur when the ground surface is subjected to erosion, excavation, or unloading, often due to glacial melting, the demolition of structures, raised water tables (Coduto 2001), compaction, or vibration (Hanna and Soliman-Saad 2001; El-Emam 2011).

Conventionally, the unit shaft resistance at failure ( $\tau_f$ ) is calculated a function of the lateral earth pressure applied on the pile and the interface friction coefficient as given in the following equation:

$$\tau_f = \sigma'_{rf} \tan \delta_f = K_s \sigma'_v \tan \delta_f = \beta \sigma'_v = K_0 (K_s / K_0) \sigma'_v \tan \delta_f \quad (1)$$

Where ( $\sigma'_{rf}$ ) is radial effective stresses at failure, ( $K_s$ ) is lateral earth pressure coefficient at failure, ( $\sigma'_v$ ) is average theoretical effective overburden pressure, and ( $\delta_f$ ) is pile-soil interface friction angle at failure. ( $\beta$ ) is a coefficient that combines the mobilized lateral earth pressure coefficient and the pile-soil friction coefficient ( $K_s \tan \delta_f$ ). ( $K_0$ ) is at-rest lateral earth pressure coefficient which can be calculated as follows:

$$K_0 = 1 - \sin \Phi' \quad (\text{Jaky 1944}) \quad (2)$$

$$K_0 = (1 - \sin \Phi') OCR^{\sin \Phi'} \quad (\text{Mayne and Kulhawy 1982}) \quad (3)$$

Where ( $\Phi'$ ) is the effective angle of shearing resistance.

It can be noted from Eq. 1 that the lateral earth pressure coefficient is presented in different forms; ( $K_s$ ), ( $\beta$ ), and ( $K_s / K_0$ ). The value of these coefficients are mostly found empirically. The ( $K_s$ ) value proposed to estimate the shaft resistance of CEDP varies widely from one researcher to another (Broms 1966; Meyerhof 1976; Coyle and Castello 1981; API 2000), and varies according to the pile material, relative density, angle of shearing resistance, and pile embedment depth. The ( $\beta$ ) value suggested to estimate the shaft resistance of CEDP also shows some variance from one researcher to another (Poulos and Davis 1980; Meyerhof 1976; Toolan et al. 1990). Similarly, different values proposed for the ( $K_s / K_0$ ) value to estimate the shaft resistance of CEDP (Kulhawy 1991; Tomlinson and Woodward 2014; Das 2011).

Despite the variation observed in the proposed lateral earth pressure coefficients ( $K_s$ ,  $\beta$ , and  $K_s / K_0$ ), these values are much lower than that needed to estimate the shaft resistance of CEDP in overconsolidated cohesionless soils. In the field, Beringen et al. (1979) performed compressive and tensile field tests on opened- and closed-ended pile load at a site with overconsolidated sand and observed that shaft resistance exceeded recommended design limits by 100–200%. More recently, Foray et al. (1998) conducted laboratory tests on piles driven in both normally consolidated and overconsolidated sand and observed that shaft resistance values of piles driven into normally consolidated sand were almost half those driven into overconsolidated sand.

The distribution of shaft resistance was long believed to increase linearly at a constant rate down to a certain embedment depth, also known as *critical depth* (Vesic 1964; Meyerhof 1976). However, recent field pile tests have dispelled that theory (Fellenius 2002; Kulhawy 1995), and researchers now attribute critical depth to the effect of the angle of shearing resistance, the fact that it decreases with depth, residual

forces, and soil arching development due to driving, and the tendency of the OCR to decrease with depth as well.

Because the overconsolidation of cohesionless soil and its variation with depth influences shaft resistance, this paper investigates experimentally the influence of such overconsolidation, its effects upon shaft resistance, the distribution of shaft resistance along the pile shaft, and the possibility of critical depth.

## 2 Experimental Investigation

A prototype experimental setup was developed in the laboratory, which consists of a tank made of thick steel (1 m long, 1 m wide, and 1.25 m deep), loading system of 25 kN capacity equipped with an AKD servo driver which allowed for strain-controlled testing, and a pile model 0.8 m long and 55 mm in diameter, to perform pile load tests in sand. The set-up can measure the total and the tip resistance of the pile, and the stresses on the pile's shaft and accordingly the total shaft resistance. Furthermore, the OCR and the stresses in the sand mass in the tank can also be measured. A schematic sketch of the set-up is presented in Fig. 1a.

Two load cells were installed at the top and the bottom of the pile model to measure the total applied load and the tip resistance, respectively. Two other load cells were placed inside the pile to measure the total load at their levels. The load cells are located at 120 mm and 240 mm from the pile base. The load cells used for this pile had a maximum capacity of 22.25 kN with an accuracy of  $\pm 0.25\%$ . Several direct shear tests were performed to establish the degree of roughness of a sandpaper to be glued to the pile shaft to maintain a ratio of interface angle to angle of shearing resistance ( $\delta/\Phi'$ ) equal to 1. As a result of those tests, Grade 150 sandpaper satisfied the unit ratio at different relative densities. Figure 1b and c show a photograph of the pile model, and a cross section for the pile model, respectively.

In the present investigation, the ratio of the distance from the pile center to the tank sides to the pile diameter ( $B/D$ ) was taken as 9.1. This ratio was sufficient to avoid any boundary effect from the sides of the testing tank (Chari and Meyerhof 1983; Shalabi and Bader 2014). Pile load tests are also affected by the mean particle size ( $d_{50}$ ) of the soil. Fioravante (2002) has suggested that the scale effect can be avoided when the ( $D/d_{50}$ ) ratio exceeds 50. In the study reported here, the ( $D/d_{50}$ ) ratio was 211.

The soil used in this experiment is commercially known as "Silica Sand 4010". The series of tests performed on this sand revealed a mean effective particle size  $d_{50}$  of 0.26 mm, a uniformity coefficient  $C_u$  of 1.88, a specific gravity  $G_s$  of 2.62, and a minimum and a maximum void ratios  $e_{min}$  and  $e_{max}$  of 0.50 and 0.84, respectively. The sand can be categorized as sub-rounded material with a peak angle of shearing resistance of  $32.96^\circ$ ,  $34.93^\circ$ , and  $36.80^\circ$  at 30%, 45%, and 60% relative density, respectively.

The pile load test performed at relative densities of 30%, 45%, and 60%. To fill up the tank up to 1.2 m height, eight soil layers of equal height were placed in the tank. To achieve the desired relative density, each soil layer were compacted. To achieve the desired relative density uniformly across the tank, preliminary tests were performed using trial and error approach where less energy (drops) was applied to the lower layers

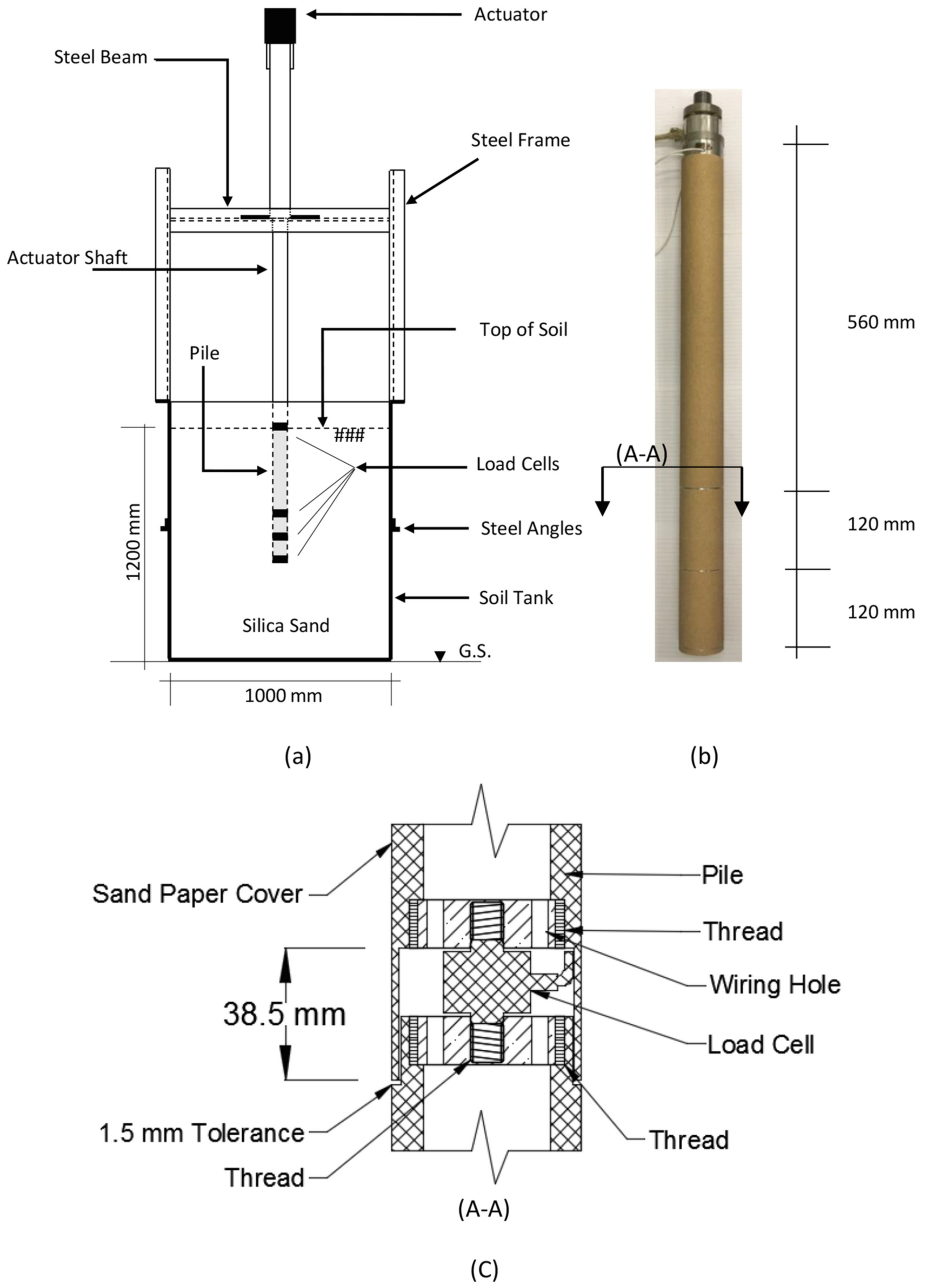


**Fig. 1.** (a) Schematic sketch of the experimental setup, (b) photograph of the pile model, and (c) section of the pile model

and more energy applied to the upper layers (Hanna and Al Khoury 2005; Hanna and Soliman-Saad 2001). The unit weight of the sand in the testing tank was measured by placing small cans of known volumes in strategic locations in the sand. Two cans were embedded in the top seven layers. Each one has a diameter of 110 mm, height of 50 mm and thickness of 3 mm. A schematic sketch for the cans arrangement and a photo of the can are presented in Fig. 2a. At the end of each test, the cans were retrieved to calculate the unit weight.

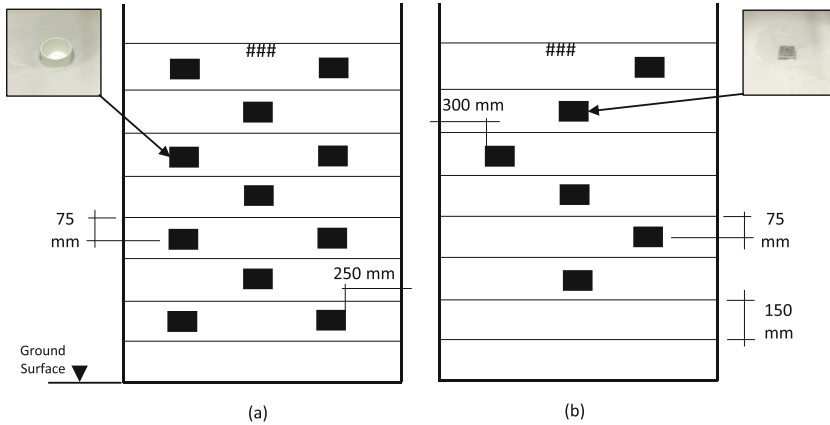
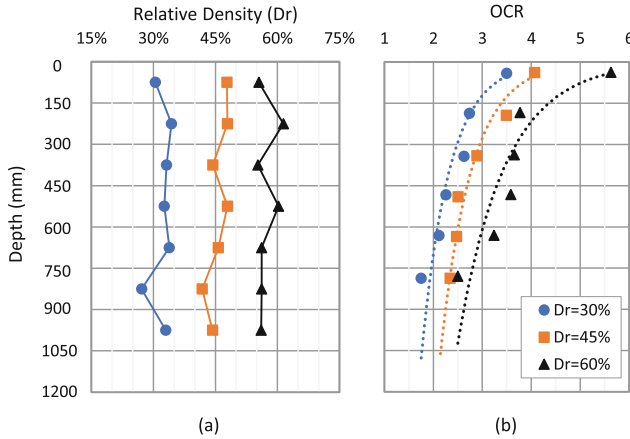


Fig. 2. (a) Unit weight can, and (b) sensors arrangement in the testing tank

The vertical stresses induced in the sand due to the compaction were measured for the first six soil layers using six sensors placed in the middle of each layer as shown in Fig. 2b. The sensors, Single Tact branded, were capacitive force sensors which differ in size according to its maximum capacity. Preliminary tests were performed to verify the readings of the sensors where the results of the sensors agreed with that obtained from a pressure load cell. Therefore, the results were recorded after each compaction test, and accordingly, the overconsolidation ratio (OCR) was calculated for each layer as follows (Hanna and Al Khoury 2005):

$$OCR = \frac{\sigma_c}{\sigma'_v} \tag{4}$$

Where ( $\sigma_c$ ) is vertical pressure at a given depth as measured by the corresponding sensor, and ( $\sigma'_v$ ) is theoretical effective overburden pressure at that depth. Figure 3a and b present the produced relative density of the sand in the testing tank and the deduced OCR values for each relative density, respectively.



**Fig. 3.** Compaction results for (a) relative density; and (b) overconsolidation ratio versus depth

To perform the pile load test, the pile was driven vertically at the center of the tank, at a rate of 25 mm/min, to the desired depth. At this stage, all sensors were set to zero, and the pile load test started when the actuator drove the pile at a rate of 5 mm/min (Le Kouby et al. 2013). The pile load test ended when the pile was displaced by 20 mm. During the test, readings of the load cells were collected continuously by the DAS. Table 1 summarizes the experimental testing program followed. A photograph taken during the pile load testing is presented in Fig. 4.

**Table 1.** Experimental testing program

Testing program			
Test No.	Relative density	Nominal depth	Depth
–	Dr	L/D	L
–	(%)	–	(mm)
1	30	5	275
2		8	440
3		10	550
4		13	715
5	45	5	275
6		8	440
7		10	550
8		13	715
9	60	5	275
10		8	440
11		10	550
12		13	715

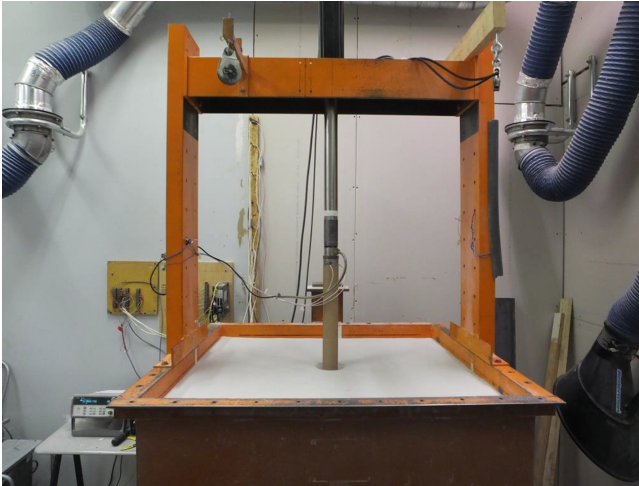


Fig. 4. Photo of pile during testing

### 3 Results and Analysis

Figure 5 presents typical test results (test 3). The total shaft resistance was found as the difference between the pile and the tip resistance. It can be noted that load-settlement curve for the total shaft resistance reached a peak value then dropped slightly as the pile displacement increased and reached a constant value at the end of the test. This behavior is in line with the results of Foray et al. (1998) for model pile tested in overconsolidated sand.

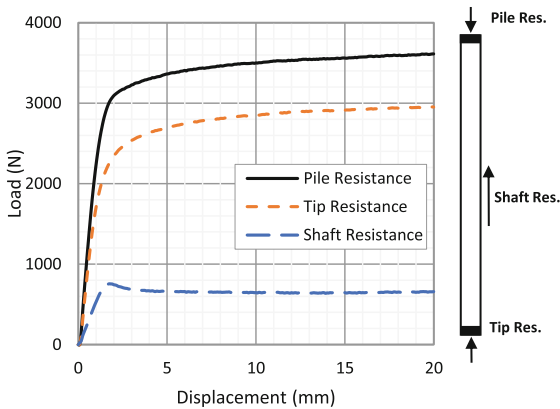


Fig. 5. Typical results (test 3): total, tip, and shaft resistance versus head displacement

Based on the load-settlement curve of the total pile resistance, the ultimate capacity was found using the tangential method. Accordingly, the ultimate shaft resistance was found. The ( $K_s$ ) was back-calculated using Eq. 1 for all the tests performed and depicted in Fig. 6. It is evident that ( $K_s$ ) values for CEDP in OC cohesionless soils have higher values than those traditionally recommended. It is noted that the ( $K_s$ ) values increased linearly with depth, and remained almost constant after nominal depth ( $L/D = 10$ ). This supports Vesic's (1967) and Meyerhof's (1976) findings that the critical depth exists when the total shaft resistance analyzed as an average even when the soil is overconsolidated. When compared to Vesic's (1967) results, as shown in Fig. 7, the critical depth appeared in overconsolidated cohesionless soils and was significantly influenced at 30% and 45% relative densities.

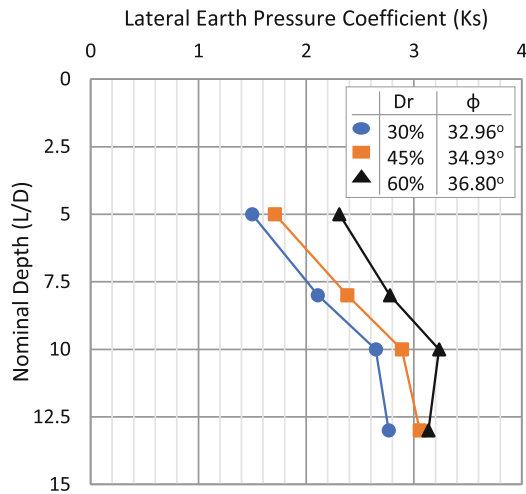


Fig. 6.  $K_s$  values versus ratio of depth to diameter ( $L/D$ )

The shaft resistance for each section of the pile was found as the difference between the two load cells at each end. Figure 8 presents typical test results (test 3) for the shaft resistance of each pile section. The load-settlement response was almost the same at the initial stages of the loading for the three sections. On the other hand, the peak shaft resistance for each section were different. The highest shaft resistance was for Sect. 1, whereas the lowest shaft resistance was for Sect. 2. This indicates a nonlinear distribution of the shear stress along the pile's shaft.

The local shear stress distribution (measured load divided by the corresponding area) on the total length of the pile model is presented in Fig. 9. The local shear stress is presented as an average value at the middle of each section. It is evident that distribution of the shear stress along the pile shaft is nonlinear. It is noted that the local shear stress for tests performed at the same nominal depth ( $L/D$ ) behave similarly where the stress value increased as the relative density increased. It is also noted that the local shear stress at a certain depth decreased as the pile depth increased which is, generally,



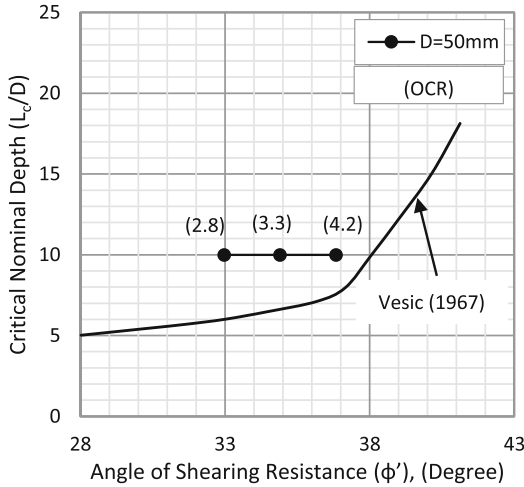


Fig. 7. Experimental critical depth results

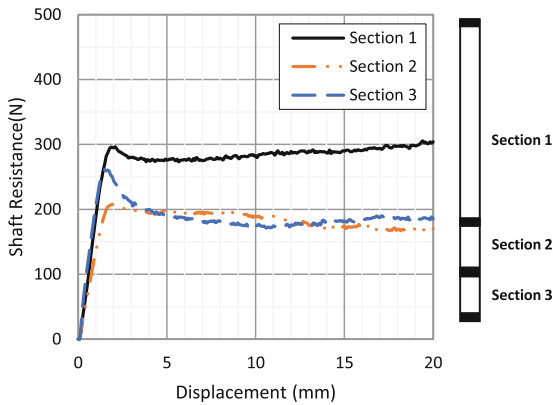


Fig. 8. Typical results (test 3): sections shaft resistance versus head displacement

in accordance with the results of Vesic (1970), Lehane et al. (1993), and Flynn and McCabe (2015). Because of this reduction, the average total shaft friction remains relatively constant as the embedment depth increases, and consequently, the critical depth appears. It can be concluded that the critical depth ( $L_c$ ) appears only when the total shaft resistance is analyzed as an average. Evidently, the critical depth appeared in overconsolidated cohesionless soils and was significantly influenced at 30% and 45% relative density.

Figure 10 presents a comparison between the test results and that found using the lateral earth pressure coefficients ( $K_s$ ,  $\beta$ , and  $K_s/K_0$ ) proposed by different authors without limiting the shear stress value. It can be noted that the shaft resistance is highly under estimated.

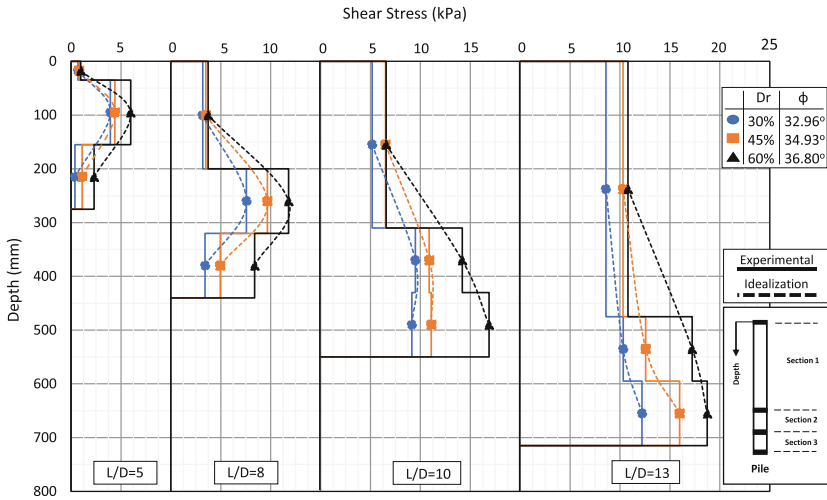


Fig. 9. Test results: shear stress on pile sections versus depth

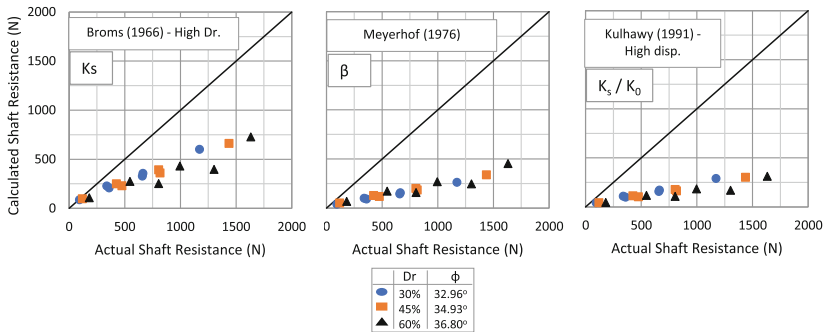


Fig. 10. Comparison between the actual and the calculated shaft resistance using values proposed by different authors

For practicality, the experimental results were correlated to the cone penetration test (CPT) end resistance ( $q_c$ ). Because the CPT was not performed, the end resistance ( $q_c$ ) was calculated according to Mayne’s (1991) equation as follow:

$$K_0 = \frac{(P_a / \sigma'_v)(q_c / P_a)^{1.6}}{145 \exp \left\{ \left[ \frac{(q_c / P_a) / (\sigma'_v / P_a)^{0.5}}{12.2 OCR^{0.18}} \right]^{0.5} \right\}} \quad (5)$$

Where ( $K_0$ ) is at rest lateral earth pressure coefficient which is calculated according to Eq. 3, ( $q_c$ ) is cone tip resistance, ( $P_a$ ) is a reference stress equal to one atmosphere (1 bar = 100 kPa), and ( $\sigma'_v$ ) is vertical effective stress. The (OCR) was found according to the experimental results presented in Fig. 3. Knowing the soil properties and the OCR values, Eq. 5 was solved to find the qc value at different levels across the testing tank at 30%, 45%, and 60% soil relative densities.

Knowing the value of shear stress and the value of the interface angle, the ( $\sigma'_{rf}$ ) value was calculated according to Eq. 1 for every section of the pile model and normalized by the average end cone resistance ( $q_c$ ) between the corresponding load cell levels to present it in unitless values. At the same nominal depth, the ( $\sigma'_{rf}/q_c$ ) values for each section at 30% relative density was close to that at the other relative densities. Accordingly, the ( $\sigma'_{rf}/q_c$ ) were averaged. Figure 11a presents the ( $\sigma'_{rf}/q_c$ ) values against the normalized distance from the pile base ( $h/D$ ). It can be noted that, for ( $h/D$ ) higher than 3.3, the ( $\sigma'_{rf}/q_c$ ) values decreased with increasing ( $h/D$ ) for piles tested at nominal depth ( $L/D = 5$ ). As the nominal depth increased ( $L/D = 8$  and 10), the ( $\sigma'_{rf}/q_c$ ) decreased at a slower rate. For nominal depth ( $L/D = 13$ ), the ( $\sigma'_{rf}/q_c$ ) increased. For

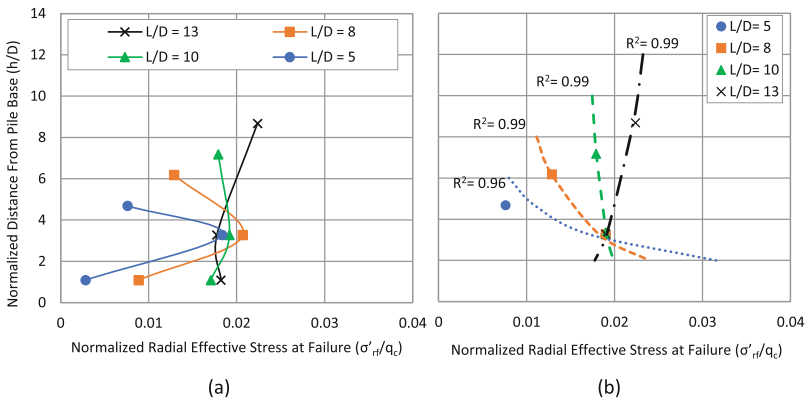


**Fig. 11.** (a) Results of ( $\sigma'_{rf}/q_c$ ) versus Ratio of ( $h/D$ ), and (b) Best fitting lines for the ratio of ( $\sigma'_{rf}/q_c$ )

( $h/D$ ) lower than 3.3, the ( $\sigma'_{rf}/q_c$ ) values decreased with decreasing ( $h/D$ ) up to a certain ( $L/D$ ) where ( $\sigma'_{rf}/q_c$ ) seemed to reach a constant value. Therefore, it can be concluded that the ( $\sigma'_{rf}/q_c$ ) values depend on the nominal depth ( $L/D$ ) ratio.

For ( $h/D$ ) higher than 3.3, the ( $\sigma'_{rf}/q_c$ ) values seem to be matched by a power function as expressed in Eq. 6. According to this equation, a regression analysis was performed, using the dataset for the twelve pile load tests, to determine the values of

factor a and b that adequately described the distribution of  $(\sigma'_{rf}/q_c)$  values along the pile shaft at different nominal depths  $(L/D)$ .

$$\left(\sigma'_{rf}/q_c\right) = a(h/D)^b \tag{6}$$

Where  $(h/D)$  is normalized distances from the pile base. The  $(\sigma'_{rf}/q_c)$  values at  $(h/D = 3.3)$  are close to each other, and accordingly, they were averaged to simplify the analysis. The values of factor a and b were found, as presented in Fig. 11b, based on the best fitting lines. Figure 12a and b present the value of “a” and “b”, respectively, versus the nominal depth  $(L/D)$ . Accordingly, the following empirical relationships were found:

$$a = 1.0843(L/D)^{-1.667} \tag{7}$$

$$b = 0.48e^{-7.372E-5(L/D)} - 4.83e^{-0.2(L/D)} \tag{8}$$

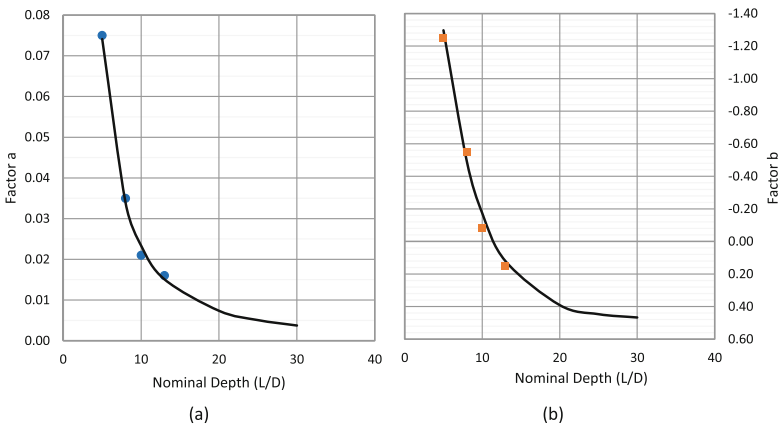


**Fig. 12.** (a) Factor a, and (b) Factor b versus the ratio of depth to diameter  $(L/D)$

For  $(h/D)$  lower than 3.3, the  $(\sigma'_{rf}/q_c)$  value was assumed to be half of that found at  $h/D = 3.3$  for nominal depth  $(L/D)$  equal to or less than 8, and same  $(\sigma'_{rf}/q_c)$  value as that found at  $h/D = 3.3$  for higher nominal depth  $(L/D)$  ratios.

The experimental results were compared to those predicted by the proposed equations. It can be noted from the comparison presented in Fig. 13 that the predicted shear stresses agree with the actual values.

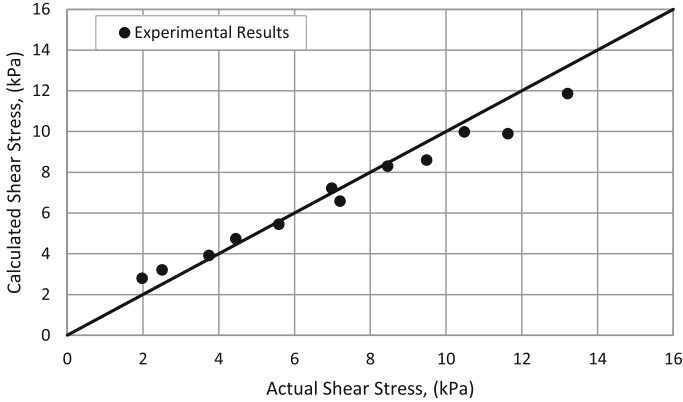


**Fig. 13.** Comparison between the actual and the calculated shaft resistance using the proposed equations

## 4 Conclusion

An experimental investigation was performed on displacement piles in overconsolidated cohesionless soil. Based on the results obtained, the following conclusions were drawn:

- 1- The shaft resistance of displacement piles increases with the increase of the overconsolidation ratio (OCR).
- 2- The lateral earth pressure coefficient ( $K_s$ ) back calculated from the total shaft resistance, were significantly higher than those traditionally recommended for displacement piles.
- 3- The critical depth ( $L_c/D$ ) appeared only when the total shaft resistance was analyzed as an average. The (OCR) increased the value of the critical depth at loose and medium dense cohesionless soils which in turn increased the shaft resistance significantly.
- 4- The shear stress distribution showed some dependency on the nominal depth ( $L/D$ ).
- 5- Empirical equations were proposed for displacement piles in overconsolidated cohesionless soils to estimate the shear stress and its distribution along the pile's shaft.

**Acknowledgements.** The first author gratefully acknowledges the financial support he received from the Saudi Arabian Cultural Bureau in Canada and the scholarship sponsored by Taif University. The financial support from the Natural Sciences and Engineering Research Council of Canada (NSERC) and Concordia University are acknowledged as well.

## References

- API: Recommended practice for planning, designing and constructing fixed offshore platforms-working stress design. 2A-WSD, 21 (2000)
- Beringen, F., Windle, D., Van Hooydonk, W.: Results of loading tests on driven piles in sand. In: International Conference of the Institution of Civil Engineers on Recent Developments in the Design and Construction of Piles, London, pp. 213–225 (1979)
- Broms, B.B.: Methods of calculating the ultimate bearing capacity of piles - a summary. *Sols-Soils* 18–32 (1966)
- Chari, T.R., Meyerhof, G.G.: Ultimate capacity of rigid single piles under inclined loads in sand. *Can. Geotech. J.* **20**(4), 849–854 (1983)
- Coduto, D.P.: *Foundation Design: Principles and Practices*. Prentice Hall, Upper Saddle River (2001)
- Coyle, H.M., Castello, R.R.: New design correlations for piles in sand. *J. Geotech. Geoenviron. Eng.* **107**(7), 965–986 (1981)
- Das, B.M.: *Principle of Foundation Engineering*. Global Engineering: Christopher M. Shortt, Cengage Learning, Boston (2011)
- El-Emam, M.: Experimental and numerical study of at-rest lateral earth pressure of overconsolidated sand. *Adv. Civ. Eng.* (2011)
- Fellenius, H.B.: Determining the resistance distribution in piles. Part 1: notes on shift of no-load reading and residual load. *Geotech. News Mag.* **20**(2), 35–38 (2002)
- Flynn, K.N., McCabe, B.A.: Shaft resistance of driven cast-in-situ piles in sand. *Can. Geotech. J.* **53**(1), 49–59 (2015)
- Foray, P., Balachowski, L., Colliat, J.L.: Bearing capacity of model piles driven into dense overconsolidated sands. *Can. Geotech. J.* **35**(2), 374–385 (1998)
- Hanna, A.M., Nguyen, T.Q.: An axisymmetric model for of ultimate capacity of a single pile in sand. *Jpn. Geotech. Soc.* **42**, 47–58 (2002)
- Hanna, A.M., Soliman-Saad, N.: Effect of compaction duration on the induced stress levels in a laboratory prepared sand bed. *Geotech. Test. J. ASTM* **24**(4), 430–438 (2001)
- Hanna, A., Al Khoury, I.: Passive earth pressure of overconsolidated cohesionless backfill. *J. Geotech. Geoenviron. Eng.* **131**(8), 978–986 (2005)
- Jaky, J.: The coefficient of earth pressure at rest. *J. Soc. Hung. Archit. Eng.* 335–358 (1944)
- Kulhawy, F.H.: Drilled shaft foundations. In: Fang, H.Y. (ed.) *Foundation Engineering Handbook*, pp. 537–552. Springer, New York (1991)
- Kulhawy, H.: Discussion of the critical depth – how it came into being and why it does not exist. *Civ. Eng. Geotech. Eng. J.* 244–245 (1995)
- Lehane, B., Jardine, R., Bond, A., Frank, R.: Mechanisms of shaft friction in sand from instrumented pile tests. *J. Geotech. Eng.* 19–35 (1993)
- Mayne, P.W.: Tentative method for estimating  $\sigma_v'$  from qc data in sands. In: *Proceedings on 1st International Symposium on Calibration Chamber Testing*, Potsdam, NY, pp. 249–256 (1991)
- Mayne, P.W., Kulhawy, F.H.: Ko-OCR relationships in soil. *J. Geotech. Eng. Div.* **108**(6), 851–872 (1982)
- Meyerhof, G.: Bearing capacity and settlement of pile foundations. *J. Geotech. Eng. Div. ASCE* **102**(GT3), 195–228 (1976)
- Poulos, H.G., Davis, E.H.: *Pile Foundation Analysis and Design*. Wiley, New York (1980)
- Randolph, M.F., Dolwin, J., Beck, R.: Design of driven piles in sand. *Geotechnique* **44**(3), 427–448 (1994)
- Shalabi, F., Bader, T.A.: Effect of sand densification due to pile-driving on pile resistance. *Int. J. Civ. Eng. (IJCE)* **3**(1), 17–30 (2014)

- Tomlinson, M., Woodward, J.: *Pile Design and Construction Practice*. CRC Press, Boca Raton (2014)
- Toolan, F.E., Lings, M.L., Mirza, U.A.: An appraisal of API RP2A recommendations for determining skin friction of piles in sand. In: *Offshore Technology Conference*. Offshore Technology Conference (1990)
- Vesic, A.S.: Investigations of bearing capacity of piles in sand. In: *Proceedings of National American Conference on Deep Foundation*, Mexico City (1964)
- Vesic, A.S.: Tests on instrumented piles, Ogeechee River site. *J. Soil Mech. Found. Div.* (1970)